

Determination of the Growth Strain of LPCVD Polysilicon

Yuping Wang, Roberto Ballarini, Harold Kahn, and Arthur H. Heuer

Abstract—This paper presents a semiempirical procedure for determining the through-the-thickness variation of the eigenstrain (eigenstrain is a generic term for any inelastic strain, including plastic strain, free thermal expansion, phase transformation, etc.) that develops during the growth of thin polysilicon films formed using low-pressure chemical vapor deposition (LPCVD). This variation is assumed to depend on the polysilicon microstructure and deposition conditions, but not on the characteristics of the (single crystal silicon) substrate. The procedure involves the use of an elastic laminated plate model to determine the eigenstrain distribution that predicts the experimentally measured substrate curvatures. In comparison to the “shaving method” presented by Ni *et al.* [1], which relies on incremental etching of a single specimen, an alternative experimental procedure is followed to measure the substrate curvatures of a series of different thickness films. While being significantly more time-consuming, the alternative procedure was expected to lead to improved predictions of the eigenstrain distribution, as it avoids the nonuniform film thicknesses produced by the etching procedure. However, a comparison of the curvature histories measured using the two approaches demonstrates that, as long as sufficiently small increments are used in the shaving method, then the improvement is insignificant. This suggests that the plasma etching does not alter the polysilicon’s intrinsic growth strain, and that the etch rate nonuniformities across the substrate are small. The eigenstrain distributions could be used, in conjunction with structural mechanics models, to design multilayered polysilicon devices with prescribed curvatures. [1175]

Index Terms—Author, please supply your own keywords or send a blank e-mail to keywords@ieee.org to receive a list of suggested keywords..

I. INTRODUCTION

As-deposited polysilicon films are generally associated with compressive or tensile residual stresses and corresponding stress gradients depending on the deposition temperature. As a result, released polysilicon structures are susceptible to undesired buckling and out-of-plane deformation. While annealing at temperatures up to 1100 °C can eliminate most of the residual stresses, there are applications for which these temperatures cannot be tolerated. An alternative to annealing is the multilayer process described by Yang *et al.* [2], in which polysilicon layers with relatively small layer thicknesses are deposited alternately at 570 and 615 °C, with tensile and

compressive stresses, respectively, to produce a composite film with the desired overall stress and stress gradient. When first developed, this process relied on empirically developed recipes (the number, thickness, and deposition temperature of each layer) to achieve desired residual stress profiles and curvatures. The trial-and-error technique used in [2] involved depositing several identical multilayers onto different single crystal silicon substrates. The average stress and stress gradient were then measured on one of these laminates; average stress was measured using substrate curvature, and stress gradients were determined by measuring the curvature (upward or downward) of cantilever beams fabricated from the multilayer. If the measurements indicated undesired results, a “correction” layer of appropriate thickness and deposition temperature was deposited onto the remaining multilayers to achieve the desired stress distribution.

To reduce the amount of empirical effort required to produce recipes for prescribed curvatures of multilayer polysilicon laminates, Ni *et al.* [1] proposed a mechanistic design approach that relies on the experimentally derived functions that define the through-the-thickness variation of the intrinsic growth eigenstrain for the two deposition temperatures. When combined with a structural analysis model (for example the finite element method, laminated plate theory, etc.) this approach could be used to develop recipes that produced prescribed residual stress distributions and their associated curvatures. This approach assumes that the stress states of early layers in the multilayer are not altered by subsequent deposition of additional layers. This assumption is supported by transmission electron micrographs [2] which show that the layers’ microstructures do not vary with the order within the multilayer. It is also assumed that the substrate is not affected by the deposition process. As will be shown in this paper, this mechanistic approach, as a result of the uncertainties associated with the physics of growth, does not lead to “exact” predictions. However, it offers a much more efficient method of producing curvatures “close” to the desired values, which can then be remedied using the previously described “correction” layers.

The first attempt at obtaining the eigenstrain-thickness functions, $\varepsilon_i^g(t)$ ($i = 570$ °C or 615 °C), made in [1] is summarized through the schematic diagrams shown in Fig. 1. ~ 500 μm thick (100) silicon substrates were oxidized at 1075°C to grow ~ 100 nm thick films of SiO₂. Thereafter, 2 μm thick (t_f in Fig. 1) LPCVD polysilicon films were deposited on both sides [Fig. 1(a)], and the polysilicon layer was stripped off one side using a chlorine plasma [Fig. 1(b)]. The 570 °C films were annealed directly after deposition for 2 h at 615 °C to ensure complete crystallization of the initially amorphous deposit.

Manuscript received October 14, 2003; revised June 7, 2004. This work was supported by the Defense Advanced Research Projects Agency under Contract N00014-00-1-0881. Subject Editor S. Mark Spearing.

Y. Wang and R. Ballarini are with the Department of Civil Engineering, Case Western Reserve University, Cleveland, OH 44106 USA (e-mail: rxb7@po.cwru.edu).

H. Kahn and A. H. Heuer are with the Department of Materials Science and Engineering, Case Western Reserve University, Cleveland, OH 44106 USA.

Digital Object Identifier 10.1109/JMEMS.2004.839003

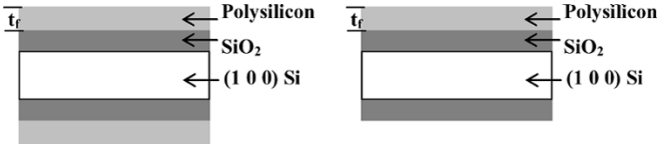


Fig. 1. Stripping of polysilicon at the backside. In [1] $t_f = 2 \mu\text{m}$, and the front side is plasma etched in 100-nm increments. In the present paper, a series of specimens with different values of t_f were fabricated.

Determination of the ε_i^g relied on the measurement of the curvature history of this $\text{SiO}_2/\text{Si}/\text{SiO}_2/\text{poly-Si}$ structure, as the polysilicon layer was etched in roughly 100 nm increments. As described in the next section, an elastic laminated plate model was used to determine the function ε_i^g that predicts the measured curvatures, and in turn the through-the-thickness residual stress profiles. The predictions made using this mechanistic approach overestimated the measured average residual stress in all but two of the devices that were fabricated using nine different recipes. The source of this discrepancy was thought to be the nonuniform ($\sim 5\%$ faster in the center) chlorine plasma etching of the front-side polysilicon. The experiments described in the next section were performed to determine whether or not the etching process in the single specimen approach presented in [1] alters the apparent intrinsic growth strain in polysilicon films or gives inaccurate results due to the nonuniform etching profile.

II. MEASUREMENT OF CURVATURE-THICKNESS RELATIONSHIPS

The through-the-thickness variations of the growth eigenstrain of polysilicon deposited at 570 and 615 °C were determined through the following procedure. A $\sim 2 \mu\text{m}$ thermal oxide layer was grown on both sides of a number of $\sim 500 - \mu\text{m}$ -thick (100) silicon wafers at 1075 °C. The curvatures K_i of the $\text{SiO}_2/\text{Si}/\text{SiO}_2$ laminates were measured using a Frontier Semiconductor Measurements (SMSi3800) laser-curvature measurement system. A nominal thickness (from 0.1-2 μm) of polysilicon was deposited on both sides of each laminate by LPCVD using SiH_4 at a flow rate of 100 sccm and a pressure of 300 mtorr; the furnace tube had an inner diameter of 225 mm. The thickness was measured using a Nanospec spectrophotometer. The polysilicon on the backside was completely etched away using a chlorine plasma (80 sccm Cl_2 , 120 sccm He, 400 mtorr total pressure, 200 W), and the curvatures of the remaining systems K_f were measured. This procedure, which involves a different wafer for each polysilicon film thickness, ensured continuous growth of each film; there were no interruptions of growth that could disturb the growth eigenstrain through the thickness, and no etching was done to reduce the thickness that might have affected the growth eigenstrain. Curvature-thickness functions were calculated for both temperatures using regression analysis.

To compare this direct approach with the shaving method presented in [1], the shaving technique was applied to the thickest polysilicon film (2 μm) deposited at 615 °C in this paper. Furthermore, to assess the residual stress predictions of the mechanistic approach, cantilever beams (2-5 μm wide and 5-1000 μm long) were also fabricated from some of the films; the fabrication procedure is summarized, as follows. Standard optical lithography was used to define the pattern in photoresist. The

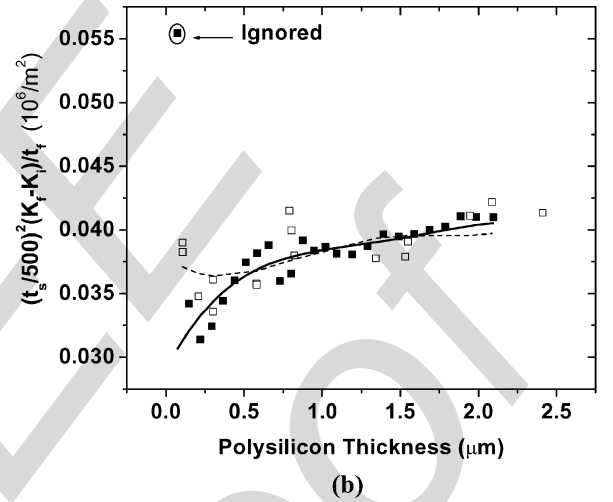
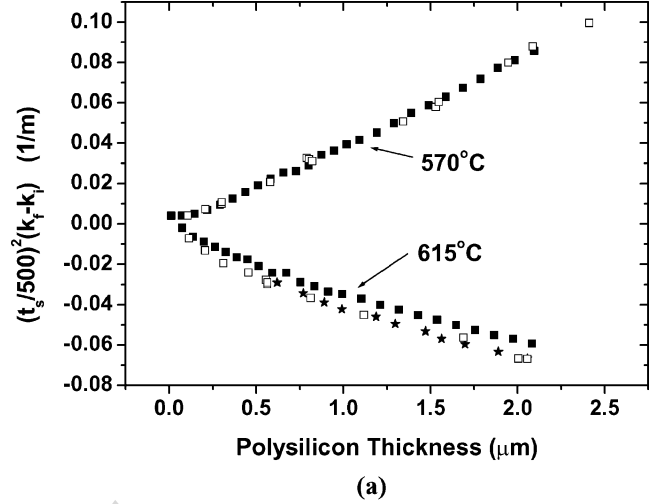


Fig. 2. Curvature change (corresponding to wafers having exactly 500- μm -thick substrates) as functions of polysilicon thickness. The filled squares and the stars were obtained using the incremental etching procedure in [1] and the present paper, respectively; the open squares were obtained using the procedure described in this paper. (a) Normalized data for polysilicon deposited at 570 and 615 °C. (b) Data for polysilicon deposited at 570 °C.

polysilicon was then etched in a chlorine plasma, and the photoresist was removed using $\text{H}_2\text{SO}_4/\text{H}_2\text{O}_2$. Finally, the SiO_2 beneath the beams was removed with a timed aqueous HF etch, and the devices were dried using supercritical CO_2 .

Fig. 2(a) presents the curvature-thickness history obtained using the different methods described above. The open squares correspond to the direct procedure (that does not involve etching), and the stars correspond to the shaving method; the filled squares are reproduced from [1]. A linear regression was performed to curve-fit the curvature versus thickness data. The functions used in subsequent calculations are

$$570 \text{ } ^\circ\text{C} \quad \Delta K = -0.0018 + 0.0499t - 0.0234t^2 + 0.0161t^3 - 0.0032t^4 \quad (1a)$$

$$615 \text{ } ^\circ\text{C} \quad \Delta K = -0.0005 - 0.0687t + 0.0427t^2 - 0.0182t^3 + 0.0029t^4. \quad (1b)$$

The functions used in Ni *et al.* [1] are

$$570 \text{ } ^\circ\text{C} \quad \Delta K = 0.0007 + 0.0301t + 0.0125t^2$$

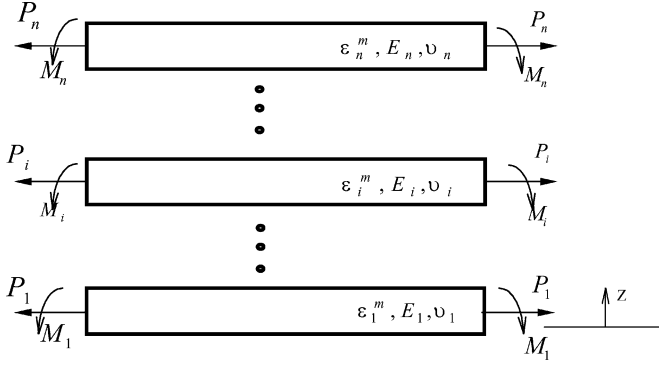


Fig. 3. Free body diagrams of individual layers of a laminated film.

$$-0.0064t^3 + 0.0014t^4 \quad (2a)$$

$$615^\circ\text{C } \Delta K = 0.0014 - 0.055t + 0.0283t^2$$

$$-0.0114t^3 + 0.0018t^4 \quad (2b)$$

where $\Delta K = (K_f - K_i)t_s^2/500^2$ is the corresponding curvature change (in dimensions of 1/m) for wafers having exactly 500- μm -thick substrates, and t_s and t are, respectively, the measured substrate thickness and the polysilicon thickness (in dimensions of μm).

For 615 $^\circ\text{C}$, there is a relative difference of up to 10% between the data taken in this paper and those reproduced from [1]. However, it is noted that the results obtained by shaving the 2 μm film in this paper [the stars in Fig. 2(a)] are in good agreement with the measurements for thinner polysilicon films (open squares). Also, the data from the as-deposited (before shaving) 2 μm polysilicon film used in [1] shows the same 10% difference from the 2 μm film used in this investigation. This indicates that the observed differences between the two sets of data for 615 $^\circ\text{C}$ polysilicon do not arise from differences in technique (shaving versus deposition of different thicknesses). As seen in Fig. 2(a), all of the data taken in this paper (open squares and stars) fall very well along a single curve, deviating by at most a few percent. This implies that the random variations due to measurement error are small, and that stochastic measurement error cannot account for the 10% discrepancy seen between this paper and that described in [1]. The possible origins for the 10% difference are a systematic error in the curvature measurement or differences in the polysilicon films deposited in [1]. This is discussed in detail in a later section.

For 570 $^\circ\text{C}$, data from the current experiment and the shaving experiment [1] are practically indistinguishable in Fig. 2(a); for clarity, the 570 $^\circ\text{C}$ data are normalized with respect to the film and substrate thicknesses, and replotted in Fig. 2(b). The dashed line shows the fourth-order polynomial fit of the data taken in this paper (open squares). In Ni *et al.* [1], the authors ignored the datum taken for the smallest thickness before performing the fourth-order polynomial fit shown as a solid line. The authors assumed that this point, which appeared to be an outlier, was an artifact of the shaving technique, probably due to the accumulated effects of nonuniform etching. As a result, while the data taken in this paper and in [1] are quite similar, there is a difference in the predictions for the behavior at small thicknesses (below 0.5 μm).

III. CALCULATION OF EIGENSTRAIN FUNCTIONS

The curvature-thickness functions were used to calculate ε_i^g through the structural mechanics model (Fig. 3) of a linear elastic laminated plate comprised of n layers, each denoted by subscript i , with thicknesses h_i , Young's moduli E_i , Poisson's ratios ν_i , and coefficients of thermal expansion α_i . In general, the internal stresses in the i^{th} layer result from the *unknown* eigenstrain due to growth within the layers, ε_i^g , and any potential difference in thermal eigenstrains, $\varepsilon_i^t = \alpha_i \Delta T_i$, between the layers. While in this paper the thermal eigenstrain is not present, the theory is presented for the general case. Thus the total eigenstrain is written as

$$\varepsilon_i^m = \varepsilon_i^t + \varepsilon_i^g. \quad (3)$$

The per unit thickness force and moment resultants in the i^{th} layer are defined as P_i and M_i , respectively. Edge effects are neglected, and an equal biaxial stress state is assumed. Force and moment equilibria of the laminate dictate that

$$\sum_{i=1}^n P_i = 0 \quad (4)$$

and

$$\sum_{i=1}^n M_i - \sum_{i=1}^{n-1} P_i \left[\frac{h_i + h_n}{2} + \sum_{k=i+1}^{n-1} h_k \right] = 0. \quad (5)$$

The moments are related to the curvatures, κ_i , through the relation

$$M_i = \kappa_i D_i (1 + \nu_i) \quad (6)$$

where $D_i = E_i h_i^3 / 12(1 - \nu_i^2)$ is the bending rigidity. Compatibility demands a constant curvature κ , and continuous axial strain along the $n - 1$ interfaces

$$\varepsilon_{i-1}^m + \frac{P_{i-1}}{E'_{i-1} h_{i-1}} + \frac{h_{i-1} \kappa}{2} = \varepsilon_i^m + \frac{P_i}{E'_i h_i} - \frac{h_i \kappa}{2}. \quad (7)$$

Equations (2)–(5) represent $2n + 1$ equations that relate the n forces, n moments, and the curvature to the through-the-thickness variation of eigenstrain (the total eigenstrains on both sides of the equation are evaluated at the interfaces).

Once the equations are solved, the discrete values of residual stress before release can be recovered as

$$\sigma_i^{res} = \frac{P_i}{h_i} + \frac{h_i E'_i \kappa}{2}. \quad (8)$$

The resulting eigenstrain and residual stress (in units of MPa) functions are obtained as

$$615^\circ\text{C } \varepsilon^m = -2 \times 10^{-6} t^4 - 0.0004 t^3 + 0.002 t^2 - 0.0032 t + 0.0015 \quad (9a)$$

$$570^\circ\text{C } \varepsilon^m = -1 \times 10^{-5} t^4 + 0.0005 t^3 - 0.0019 t^2 + 0.0018 t - 0.003 \quad (9b)$$

$$615^\circ\text{C } \sigma^{res} = 0.4201 t^4 + 84.797 t^3 - 412.44 t^2 + 656.96 t - 529.48 \quad (10a)$$

$$570\text{ }^{\circ}\text{C } \sigma^{res} = -0.0276t^4 - 96.271t^3 + 371.62t^2 - 367.82t + 379.46. \quad (10b)$$

The corresponding functions obtained by Ni *et al.* [1] are

$$615\text{ }^{\circ}\text{C } \varepsilon^m = -5 \times 10^{-6}t^4 - 0.0002t^3 + 0.0012t^2 - 0.0021t + 0.0009 \quad (11a)$$

$$570\text{ }^{\circ}\text{C } \varepsilon^m = 6 \times 10^{-6}t^4 - 0.0002t^3 + 0.0008t^2 - 0.001t - 0.0022 \quad (11b)$$

$$615\text{ }^{\circ}\text{C } \sigma^{res} = 1.0586t^4 + 49.501t^3 - 254.06t^2 + 431.76t - 420.97 \quad (12a)$$

$$570\text{ }^{\circ}\text{C } \sigma^{res} = 0.2059t^4 + 41.317t^3 - 145.98t^2 + 198.52t + 216.23. \quad (12b)$$

IV. ASSESSMENT OF THE GROWTH EIGENSTRAIN FUNCTIONS

Figs. 4 and 5 compare the growth eigenstrain and residual stress distributions calculated in this paper and in [1]. Although there was a 10% difference in the measured curvature change for the 615 °C polysilicon films, the calculated stress and eigenstrain profiles are quite similar for the 615 °C polysilicon films used in this paper and in [1]. However, as discussed above, the shape of the calculated stress and eigenstrain profiles show distinct differences at small thicknesses. At low thicknesses, Ni *et al.* [1] predict an increase in the tensile stress with thickness, while this paper predicts a decrease in tensile stress with thickness for polysilicon films deposited at 570 °C. To determine which eigenstrain functions are qualitatively correct, cantilever beams were fabricated from two polysilicon films for both deposition temperatures. If the shape of the eigenstrain profile obtained in this paper is correct, the cantilever beams fabricated from the 570 °C polysilicon should bend downward upon release (upon release the top surfaces of the beams will end up in a higher tension than the bottom), while if the eigenstrain profile predicted in [1] is correct, the beams should bend upward. For the 615 °C polysilicon, the functions derived in this paper and in [1] both predict that the cantilevers will bend upward upon release.

Fig. 6 shows that upon release 0.82- μm -thick 570 °C cantilever beams bend downward, suggesting that the associated function calculated in this paper is at least qualitatively correct for small thickness films, while the one derived in [1] is not. While they are not shown here, all of the 615 °C beams bend upward. Although not explored in this paper, cantilever beams can also be used to check the uniformity of the layer stress state across the substrate.

The mechanistic model was assessed further by comparing its predictions for curvature upon release of the cantilever beams. Due to the large out-of-plane deformation, the curvatures of the released beams were measured using a “focusing” method, where the objective lens of an optical microscope is moved to focus first on the bottom of the anchored side of the beam and then to focus on the tip of the free side to estimate the

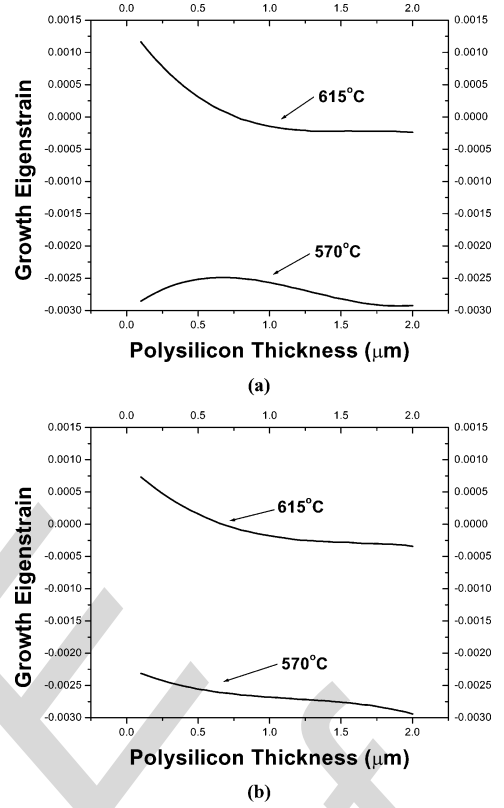


Fig. 4. Calculated growth eigenstrain profiles from (a) this paper. (b) [1].

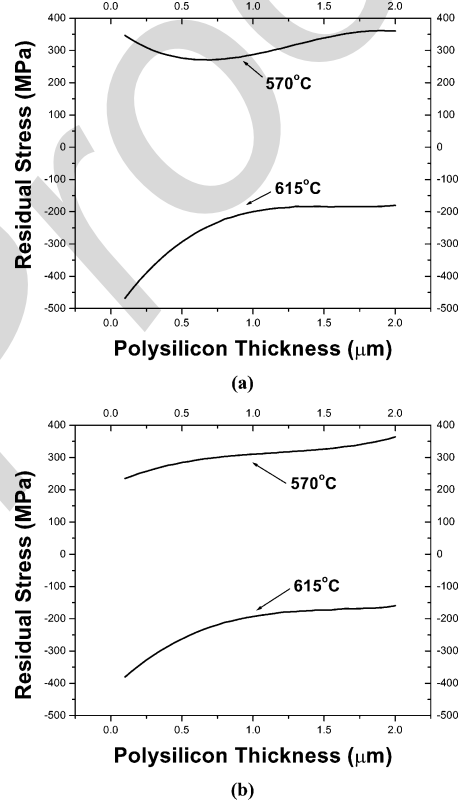


Fig. 5. Calculated residual stress profiles from (a) this paper. (b) [1].

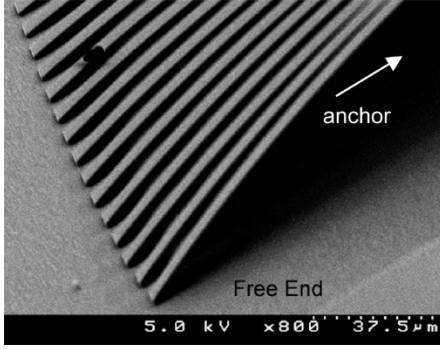


Fig. 6. 0.82- μm -thick cantilevered polysilicon beams deposited at 570 $^{\circ}\text{C}$ bend downward; the free tip touches the substrate.

out-of-plane deformation. The radius of curvature is calculated by solving the following two equations

$$2R \sin^2\theta = \Delta \quad (13)$$

$$2R\theta = L \quad (14)$$

where R , θ , Δ , L are defined in Fig. 7.

The bending deformation is constrained once the tips of the beams touch the substrate, as shown in Fig. 6. However, knowing the distance between the bottom of the beam and the substrate (the etched SiO_2 thickness), and checking if the tip hits the substrate for beams with different lengths, a bound on the released curvature could be obtained. For example, for the 570 $^{\circ}\text{C}$ beams with thickness of 1.34 μm , the tip of the 85 μm -long beam touches the substrate, while the 80 μm long beam does not. Also, the effect of the lateral etching of the oxide underlying the anchor side during the isotropic HF release etching is accounted for by adjusting the beam length by an additional 5 μm .

The predicted and measured radii of curvature (or curvature bounds) are listed in Table I; the error of the experimental measurements is $\pm 2\%$. The predicted and measured curvatures all have the same sign and are roughly of the same order of magnitude. The thinner 570 $^{\circ}\text{C}$ beams have smaller radii of curvature than the predicted values. This emphasizes the fact that the inaccuracies in absolute measurements are greatest for the smallest thicknesses.

The high curvature of the thinner 570 $^{\circ}\text{C}$ beams indicates that the polysilicon at the bottom of the film – the material that was deposited first – contains a higher tensile stress than expected. The stress of this region is predicted using the curve fit to the substrate curvature measurements as a function of film thickness shown in Fig. 2(a). The anomalous stress level could be the result of a difference in the origins of the residual stress of this region. At these temperatures (≤ 615 $^{\circ}\text{C}$), no stress relaxation is expected [2] as the film growth progresses. Tensile stresses in LPCVD polysilicon are essentially caused by the density increase that accompanies crystallization from an as-deposited amorphous material [2], [3]. However, for Volmer-Weber films (films that initially grow by the nucleation of discrete islands that enlarge and coalesce into a continuous film, which then thickens) very high tensile stresses occur when the islands coalesce in the early stages of deposition [4]. This could be the origin of the high tensile stress at the bottom of the 570 $^{\circ}\text{C}$ films

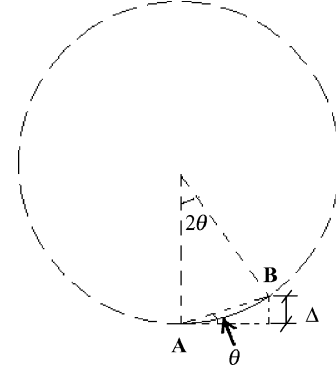


Fig. 7. Focusing method for measuring curvature. The solid arc of AB is the bent beam, L is the length of the beam.

TABLE I
COMPARISON OF THE EXPERIMENTALLY MEASURED CURVATURES OF RELEASED BEAMS WITH THOSE PREDICTED BY THE MECHANISTIC MODEL

Film Thickness (μm)	Deposition Temperature ($^{\circ}\text{C}$)	Released Radius of Curvature (m)	
		Predicted	Measured
0.82	570	-0.17e-2	>-0.15e-3
1.34	570	-0.80e-2	[-0.2e-2, -0.18e-2]
0.56	615	0.45e-3	0.36e-3
1.12	615	0.70e-3	0.75e-3

and the high observed curvature. Whatever the origin, this result indicates that special care must be taken to accurately predict the growth eigenstrains at very small thicknesses. One obvious improvement over the current practice would be to include the stress gradient data obtained for the released cantilever beams (Table I) in the formulation of the eigenstrain profiles.

V. SOURCES OF INACCURACIES

In this section, we analyze the errors or inaccuracies involved in this experimental procedure and estimate bounds on the resulting inaccuracy of residual stress or curvature prediction of the final multilayer systems. For the purpose of simplicity, the error in the residual stress is estimated by adding up all the errors involved in the measurement of thickness, curvature, etc., according to the Stoney equation $\sigma^{res} = (E/(1-\nu))(t_s^2/6t_f)(K_f - K_i)$, as follows:

1) Inaccuracy of the polysilicon thickness t_f : although the LPCVD deposition of polysilicon is supposed to be uniform, the thickness near the edge is usually larger than that of the center area (in the most serious cases, the outer 5% area can have thickness 20% larger than the center). Moreover, in our furnace, the deposition rate at the center varies for different runs, up to $\pm 3\%$. The inaccuracy in measuring the polysilicon thickness using the spectrometer is assumed to be $\pm 2\%$; 2) The measurement of substrate thickness t_s is accurate to $\pm 1\%$; 3) The inaccuracy of the measurement of the curvature ($K_f - K_i$) is about $\pm 1\%$ (larger for small curvature); 4) The effect of overetching or

etching nonuniformities in the backside silicon stripping. When removing the backside polysilicon, the center material clears first, and, thus, this area was overetched to clear the edge material. The error in curvature due to this effect is assumed to be about $\pm 3\%$. (For the 570°C polysilicon, underetching the backside polysilicon will leave a small amount of tensile material on the backside, and overetching will remove a small amount of compressive material (the thermally grown oxide) on the backside. Therefore, the error in $(K_f - K_i)$ for 570°C polysilicon can only be negative.)

As discussed above, the combined effects of the random measurement errors must be small, since the data are so well behaved. The error due to the backside polysilicon overetching must also be small, since the measurement of the $0.5\ \mu\text{m}$ 615°C film agrees well with the $2\ \mu\text{m}$ 615°C film shaved back to $0.5\ \mu\text{m}$, even though the backside etching time (and consequent overetching) for the $2\ \mu\text{m}$ film was necessarily four times that of the $0.5\ \mu\text{m}$ film. Therefore, since no systematic errors can be identified, the 10% discrepancy between the curvature changes seen in Fig. 2(a) for the 615°C polysilicon films used in this paper and for the 615°C film used by Ni *et al.* [1] must originate with the films themselves. It is clear from Fig. 2(a) that all 15 films deposited at 615°C in this paper display the same residual stress profile, but the stress profile of the one film used by Ni *et al.* [1] is different. While the same LPCVD furnace was used for all films shown in Fig. 2, approximately one year passed between the experimental work of Ni *et al.* [1] and this investigation, and maintenance during that year included replacement of the furnace tube and mass flow controllers and recalibration of the thermocouple temperature sensors. As discussed in Yang *et al.* [2], the origin of the compressive stresses in polysilicon deposited at high temperatures is not well understood. It is possible that a small change in deposition conditions, such as temperature or gas flow, could result in a 10% difference in the residual stress profile. We, therefore, recommend that the residual stress profiles of films produced by particular equipment be periodically checked, especially after major hardware changes.

For the prediction of the eigenstrain functions, the fitting procedure used for the curvature history curve induces another possible error of $\pm 2\%$ (even larger for the small thicknesses) due to the fact that the fitting curve does not pass through all the data exactly. Thus the final estimated residual stress for the single layer system is accurate within a few percent. In considering a multilayer system, the average residual stress is roughly $\sum_i t_i \sigma_i / \sum_i t_i$, in which t_i and σ_i are the thickness and average residual stress of the i^{th} layer. The overall achievable accuracy in the final multilayer residual stress design can be controlled around $\pm 3\%$ of the magnitude of the residual stress of the single temperature polysilicon layer (i.e., $\pm 9\ \text{MPa}$ for a typical single-layer stress of $300\ \text{MPa}$), not the same percentage error of the final averaged residual stress of the multilayer. In addition, there is a variability in the deposition rate of about $\pm 3\%$. This inaccuracy did not play a role in the above measurements, when the film thicknesses were measured after deposition. However,

in making predictions for the stresses of films to be deposited, it must be taken into account.

As a demonstration of the predictive capabilities provided by this paper, a two-layer system, i.e., a layer of $0.82\ \mu\text{m}$ (570°C) followed by another layer of $0.56\ \mu\text{m}$ (615°C), which is predicted to yield an average stress of $22\ \text{MPa}$ was deposited. The measured value of $27\ \text{MPa}$ roughly matches the prediction, and the mismatch is within the inaccuracies discussed above.

VI. SUMMARY AND CONCLUDING REMARKS

This paper indicates that the shaving technique for determining eigenstrain functions for deposited films is adequate and does not alter the stress state of deposited polysilicon films. However, for very small thicknesses, it is more accurate to deposit thin films and measure their behavior directly. Even for this technique, however, the stress gradient of very thin films is not accurately predicted. It is suggested that the curvatures of released cantilever beams fabricated from these films be used as inputs to help refine the eigenstrain functions. For those beams that bend downward after release, etching holes through the Si substrate would allow enough space for the beams to achieve their equilibrium shapes.

The inaccuracies of the predictions made using this technique are limited to a few percent in the stress of a single layer. However, for multilayers that are designed to have small overall stresses ($< 10\ \text{MPa}$) compared to the stresses of individual layers ($\sim 300\ \text{MPa}$), this uncertainty can be a significant fraction. The trial-and-error technique followed by Yang *et al.* [2] can still be followed to adjust the total residual stress to be close to the desired values.

REFERENCES

- [1] A. Ni, D. Sherman, R. Ballarini, H. Kahn, B. Mi, S. M. Phillips, and A. H. Heuer, "Optimal design of multilayered polysilicon films for prescribed curvature," in *J. Mater. Sci.*, W. O. Soboyejo, R. Ballarini, and S. M. Allameh, Eds., *The Mechanical Properties of MEMS Structures*, to be published.
- [2] J. Yang, H. Kahn, A. He, S. M. Phillips, and A. H. Heuer, "A new technique for producing large-area as-deposited zero-stress LPCVD polysilicon films: The multipoly process," *J. Microelectromech. Syst.*, vol. 9, pp. 485–493, 2000.
- [3] H. Kahn, A. Q. He, and A. H. Heuer, "Homogeneous nucleation during crystallization of amorphous silicon produced by LPCVD," *Philosoph. Mag. A*, vol. 2, pp. 137–165, 2002.
- [4] J. A. Floro, E. Chason, R. C. Cammarata, and D. J. Srolovitz, "Physical origins of intrinsic stresses in Volmer-Weber thin films," *MRS Bull.*, vol. 27, pp. 19–25, 2002.



Yuping Wang received the B.S. degree in engineering mechanics from Tsinghua University, China, and the Ph.D. degree in civil engineering from Case Western Reserve University, Cleveland, OH, in 2003. Her graduate research involved theoretical and computational modeling of cracks in heterogeneous solids, as well as fabrication, testing and analysis of polycrystalline silicon MEMS devices.

Upon graduation, she joined ABAQUS, Inc. as a development engineer.



Roberto Ballarini received the B.E. degree from City College of New York in 1980, and the M.S. and Ph.D. degrees in 1981 and 1985, respectively, from Northwestern University, all in civil engineering.

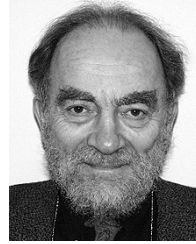
He joined the Department of Civil Engineering, Case Western Reserve University, Cleveland, OH, in 1986 as an Assistant Professor and is currently the Leonard Case Jr. Professor of Engineering. He is recognized for his research and teaching accomplishments in the general area of fracture mechanics, the mechanics and materials science of MEMS, and the

mechanics of biological composites. He held visiting professor positions with the Politecnico di Torino, Università di Pisa, and the University of Minnesota.



Harold Kahn received the B.S. degree in metallurgical engineering from Lafayette College, Easton, PA, in 1985 and the Ph.D. degree in electronic materials from the Department of Materials Science and Engineering, Massachusetts Institute of Technology, Cambridge, in 1992.

He is currently a Researcher Associate Professor with the Department of Materials Science and Engineering, Case Western Reserve University, Cleveland, OH. His research interests include wafer-level mechanical testing of surface-micromachined materials and nanostructured biological materials, and shape-memory actuated microfluidic devices.



Arthur H. Heuer received the B.S. degree in chemistry from the City College of New York in 1956 and the Ph.D. degree in applied science and the D.Sc. degree in physical ceramics, both from the University of Leeds, in 1966 and 1977, respectively.

He joined the Department of Materials Science and Engineering, Case Western Reserve University, Cleveland, OH, in 1967 as an Assistant Professor and is currently University Professor and Kyocera Professor of Materials Science. He is world renowned for his research accomplishments on phase transfor-

mations in ceramics and intermetallics, transmission electron microscopy of defects in materials, high-resolution electron microscopy studies of interfaces in advanced structural composites, dislocations in ceramics, biomimetic processing of ceramics, rapid prototyping of engineering materials, materials science of MEMS, and surface hardening of stainless steels and titanium alloys.

Dr. Heuer served as Editor of the *Journal of the American Ceramic Society* from 1988 to 1990. He was elected to the National Academy of Engineering in 1990 and was made an external Member of the Max-Planck Institute for Materials Science, Stuttgart, Germany, in 1991.

LEEEF
PROOF